

1 **Title:** Morphological change induced with NaOH-water solution for ramie fiber: change mechanism
2 and effects of concentration and temperature

3

4 **Authors:** Takato Nakano^{1*}, Takashi Tanimoto², Tsuginosuke Hashimoto¹

5

6 **Affiliation:**

7 1: Laboratory of Biomaterials Design, Division of Forest and Biomaterials Science, Graduate School of
8 Agriculture, Kyoto University

9 2: Asahi woodtech company

10 Chuoh-ku, Osaka, 541-0054, Japan

11

12 **Address:**

13 1: Kita-Shirakawa, Kyoto, 606-8502 Japan

14 2: Chuoh-ku, Osaka, 541-0054, Japan

15

16 ***: Corresponding author**

17 **e-mail:** tnakano@kais.kyoto-u.ac.jp

18 **Phone and Fax:** +81-75-753-6234

19

20

21 **Abstract:**

22 The morphology of ramie fiber treated with NaOH-water solutions at various concentrations was
23 observed with an epi-illumination microscope (EIM) equipped with a charge-coupled device (CCD)
24 camera. The crystallinity was measured by X-ray diffraction. The morphological changes in length
25 and width were quantified using image analysis. Changes in morphology were noted for samples
26 treated with NaOH-water solutions at room temperature in the narrow concentration range of $0.08 <$
27 $[\text{NaOH}] \leq 0.12$. For samples cooled at -5°C after treatment, the morphological changes started at a
28 lower concentration, i.e., at $[\text{NaOH}] = 0.05$. The change was observed as contraction in length and
29 swelling in width. The mechanism for this dimensional change related closely not to the conformation
30 of the whole microfibril but to the crystallinity of cellulose chains that had been de-crystallized by the
31 NaOH-water solution: the calculated bond angle was too small for a zigzag conformation of the whole
32 microfibril.

33

34 **Keywords:** Morphology, NaOH-water solution, Crystallinity, Cellulose microfibril, Contraction,
35 Conformation

36

37

38 **Introduction**

39 Cellulose is the main constituent of wood and other plants, serving to maintain their structures and
40 provide various physical properties. It is the greatest sustainable bioresource on earth. Native
41 cellulose has a high crystallinity and is mostly found in plant cell walls as aggregates of cellulose
42 microfibrils. These microfibrils have recently been categorized as nanofibers or nanocrystals [1]. In the
43 present study, we quantified the morphological changes that occurred during treatment of ramie
44 microfibrils with NaOH-water solution.

45 Native cellulose contains two crystalline forms, i.e., Ia and Ib. These forms can be
46 transformed into other crystalline forms, such as cellulose II, via treatment with NaOH-water
47 solution. Such polymorphic transformations have been discussed by many researchers [2-9].
48 O'Sullivan [10] attempted to bring and examine previous studies on cellulose structure over past few
49 decades. The dissolution mechanism of cellulose during NaOH treatment has been studied by nuclear
50 magnetic resonance (NMR) spectroscopy [11, 12]. Recently, Cai et al. [13-15] applied the method of Roy
51 et al. [16] to the NaOH/urea and LiOH/urea systems. The latter authors used calorimetry, small X-ray
52 scattering, and viscometry to study the structure of NaOH-water and cellulose-NaOH-water solutions
53 in the range of various concentration, and proposed a mechanism that was appropriate at lower
54 temperatures.

55 The morphological changes of cellulose that occur with NaOH-water treatment have been
56 known for a long time. Davidson [17] and Sobue et al. [18] reported the effects of both concentration
57 and temperature on qualitative changes in morphology. Watanabe et al. [19] also observed

58 crystallinity changes at low temperatures. Moigne et al. [20, 21] studied the morphological and
59 swelling properties of native and regenerated cellulose from the viewpoint of cellulose solubility using
60 water-soluble solvents such as NMMO (N-methylmorpholine-N-oxide). Although the crystalline
61 transformations and dissolution of cellulose in alkali have been extensively studied, the quantitative
62 evaluation of the morphological changes of the fibers during de-crystallization treatment has rarely
63 been discussed, and its mechanism is poorly understood.

64 Stöckmann [22, 23] first reported the changes in morphology of wood pulp that occurred
65 when it was treated with NaOH-water solutions and proposed a mechanism. Nakano [24, 25],
66 Ishikura and Nakano [26], and Tanimoto and Nakano [27, 28] reported changes in the dimensional
67 and mechanical properties of wood that occurred after treatment with NaOH-water solution; they
68 attributed these changes to morphological changes in the microfibrils in the wood cell walls. Their
69 results were later confirmed by Voronova et al. [29] and Ray and Sarkar [30]. Although many studies
70 concerning treatments of wood and cellulose with NaOH-water solution have been reported, a
71 quantitative description of the morphological changes of the microfibrils and fibers after treatment,
72 particularly with respect to conformational changes, has not been reported to our knowledge.

73 The next subject of this work was to obtain quantitative, fundamental information on the
74 conformation of microfibrils treated with NaOH-water solution. A goal was to model these
75 conformational changes that occur during such treatment; the modeling and simulation results will be
76 reported in a separate publication. Nishiyama et al. [31] and Sao et al. [32] examined the morphology
77 of alkali-treated ramie in detail, but they focused on the changes in crystal structure and did not

78 establish a relationship between the macroscopic morphology and the conformation of the amorphous
79 cellulose chains which is the structural arrangement. Thus, in the present work, conformational
80 changes in the cellulose chains and in the whole microfibrils are discussed for ramie fiber partially
81 de-crystallized by treatment with NaOH-water solution. These conformational changes were inferred
82 from changes in their macroscopic morphologies and crystallinities.

83

84 **Experimental**

85 Materials and sample preparation

86 Purified ramie (commercial grade) was donated by Nichimen Kyokai. Samples of 10 ramie fibers cut
87 about 2 mm long were treated with NaOH-water solution of different concentrations. The change in
88 morphology of a sample was observed using an epi-illumination microscope (EIM) (Nikon Optiphot,
89 Tokyo, Japan) equipped with a charge-coupled device (CCD) camera. The magnification of the image
90 was determined by a scale in the image; the magnification of the objective lens was always $5\times$.

91 To confirm the morphological changes in detail, the ramie fibers were continuously treated
92 with NaOH-water solution at concentration fractions increasing from 0.00 to 0.20 (Experiment I). The
93 same procedure was repeated several times to confirm reproducibility. In Experiment I, a sample was
94 placed in distilled water and allowed to stand overnight at room temperature. The sample was then
95 placed on a glass slide and excess liquid was removed. The sample was observed with the EIM and the
96 CCD camera. After observation, the sample was placed in NaOH ($[\text{NaOH}] = 0.03$) and then allowed to
97 equilibrate overnight at room temperature. This sample was observed by the EIM with the CCD

98 camera for a second time. The process was repeated with increasing NaOH concentration for [NaOH]
99 ranging from 0.00 to 0.20. In this experiment, the immersion time increased with exposure to higher
100 concentrations because the same sample had been exposed consecutively in solutions of increasing
101 concentration.

102 Two other experiments (Experiments II and III) were conducted to observe the dependence
103 of the morphology of the ramie fiber on NaOH concentration. In Experiment II, the sample was placed
104 in NaOH-water solution at various concentration fractions ranging from 0.00 to 0.20 and was then
105 allowed to stand for 1 week at room temperature. This sample was observed by EIM. After
106 observation, the sample was rinsed for 1 week with distilled water and then observed again. In
107 Experiment III, after the above NaOH treatment, the sample was held at -5°C for 1 day and then
108 rinsed with distilled water for 1 week. Observation by EIM in Experiment III was done before and
109 after the -5°C cooling treatment and after rinsing.

110 Overall, 15 conditions with 8 to 10 samples per [NaOH] condition were studied.

111

112 Measurement of morphological changes

113 Digital EIM images were transferred to a computer where Photostitch (Canon Co., Ltd.) and ImageJ
114 (freeware) image analysis software were used to measure the lengths and widths of the ramie fibers.

115 The length of a ramie fiber was calculated as the sum of the distances between points along its length.

116 The width was calculated as the average of five locations where the fiber was not twisted.

117

118 Crystallinity

119 Samples that were cut to shorter lengths were treated with NaOH-water solutions at various
120 concentrations by the above procedures, then rinsed with distilled water for 1 week, and oven-dried at
121 50°C under vacuum for 1 day. Pellets of approximately constant density were made from these
122 samples using a molding machine. Diffraction patterns were obtained for these pellets at room
123 temperature using an X-ray diffractometer (Rigaku Ultima IV) operating at 40 kV and 40 mA over a
124 scanning range of 5–35° and at a scanning speed of 2°/min.

125 The crystallinity based on the X-ray diffraction measurement is generally calculated as the
126 ratio of the intensity of crystalline cellulose to the total intensity or their area ratio. However, it is
127 difficult to define the extent of conversion in crystalline region for both cellulose I and II using the
128 same procedure because there is remarkable change in the profile and the effect of crystallite size on
129 crystallinity index. Thus, some methods have been proposed [33]. Revol et al. [34] reported the effect of
130 mercerization on crystallite size and crystallinity index. French and Cintron [35] also pointed out the
131 effect of crystallite size on the Segal crystallinity index. The effect appears to be remarkable in the
132 lower crystallinity estimated by the Segal method.

133 We examined some X-ray methods containing the Segal method and compared them with
134 ¹³C CP/MAS NMR method [36] where the crystallinity is calculated by expressing the area of the peak
135 at 89 ppm as a ratio of the total area assigned to cellulose-C4. The X-ray method highly correlated
136 with the NMR method was adopted, which had good agreement in the whole [NaOH] region
137 containing the transformation region from cellulose I to cellulose II [37]: the coefficient of

138 determination was 0.869. The method estimates the crystallinity as below. The total intensity I_t and
139 the amorphous intensity I_a were confirmed from the peak height of the diffraction (200) and the
140 height of an intersection point where the perpendicular line through the peak (200) crosses the
141 straight line passing the specified point and $2\theta = 30^\circ$, respectively: the specified point is the minimum
142 2θ between (1-10) and (200) for cellulose I and between (110) and (1-10) for transformation from
143 cellulose I to II and cellulose II. Then, the crystallinity was calculated using equation $(I_t - I_a)/I_t$.

144

145

146 **Results and discussion**

147 Morphological changes for non-cooled samples

148 **Figure 1(a)** shows the changes in the morphology of the ramie fiber as a function of NaOH
149 concentration. Few changes were observed for $[\text{NaOH}] \leq 0.05$. A slight twist and contraction was
150 observed near $[\text{NaOH}] = 0.10$, while the width remained unchanged. However, significant changes in
151 length, width, and twist occurred for $[\text{NaOH}] > 0.10$.

152 The changes in length and width averaged over 8–10 samples are indicated by open circles
153 in **Figure 2(a) and (b)**, respectively. Their dimensions were accurately determined using image
154 analysis. Changes in the ramie fiber morphology, i.e., decreasing length and increasing width,
155 occurred over a narrow range of NaOH concentrations, i.e., $0.08 \leq [\text{NaOH}] \leq 0.12$. These changes
156 corresponded to changes in the crystallinity (open circles in **Figure 3**). This $[\text{NaOH}]$ range is similar to
157 that reported by Kamide et al. [38] and Yamane et al. [39]. No changes were observed at $[\text{NaOH}] <$

158 0.05 and $[\text{NaOH}] > 0.12$.

159 Although the concentration dependence (**Figure 2(a)**) was similar to those reported for
160 dimensional changes in the longitudinal direction of wood samples [25, 40, 41], the onset of the
161 changes was different. Contraction of a ramie fiber started at $[\text{NaOH}] = 0.08$, while for wood, it began
162 at a higher concentration of $[\text{NaOH}] = 0.10$. Additionally, changes in the ramie fiber leveled off at
163 $[\text{NaOH}] > 0.12$; this was not observed with wood.

164 In this study, the contraction of a ramie fiber treated with NaOH-water solution reached
165 nearly 0.30 point (**Figure 2(a)**), much greater than the reported 0.07 for wood [36, 40]. This substantial
166 difference is attributed to large structural differences. Microfibrils of ramie fiber are almost free in the
167 sense that they are not strongly restricted by other components, while microfibrils of wood are
168 embedded in a matrix such as hemicellulose and lignin. Moreover, the latter forms a helical structure
169 in the cell wall. In this connection, contraction of fibrillated cells reached 0.20 point after treatment
170 with NaOH-water solutions [42]. Revol and Goring [2] and Murase et al. [3] noted that lignin, which is
171 layered between microfibrils, limits the flexibility of cellulose chains and thereby the transformation of
172 cellulose I to cellulose II. The results shown as open circles in **Figure 2(a)** and **Figure 3** suggested that
173 the remarkable changes in morphology with NaOH treatment were closely related to crystallinity.

174 The concentration dependence of the morphological changes in fiber length and width after
175 rinsing is shown as closed circles in **Figures 2(a) and (b)**. After rinsing, the length barely changed,
176 while the width decreased markedly. However, the swelling in width remained at 0.30 point with
177 $[\text{NaOH}] \geq 0.12$ even after rinsing. Both the induced contraction and residual swelling at the same

178 [NaOH] are attributed to the effect of an amorphous region created by the NaOH treatment. The
179 mechanism is discussed below.

180

181 Effect of cooling on morphological changes

182 The effect of cooling on morphological changes was examined in Experiment III. The effect of cooling
183 on the cellulose structure in cellulose-NaOH-water solution has been described by others. Davidson
184 [17] and Sobue et al. [18] observed the morphological changes and temperature dependence. Roy et al.
185 [16] examined in detail the structure in solution using various methods, such as small-angle X-ray
186 diffraction, viscosity, and differential scanning calorimetry (DSC) at low temperatures (-60 to 0°).
187 They proposed a model in which the cellulose-NaOH-water solution was composed of soda hydrates
188 bound to cellulose, with a “core” of nine free soda hydrates and free water. The solubility and swelling
189 of alkali-treated cellulose (e.g., by NaOH or LiOH) and NaOH/urea-water solutions are temperature
190 dependent, especially at low temperatures. Qi et al. [43] reported that the solubility of cellulose in such
191 solutions is strongly temperature dependent and that cellulose with a molecular weight of 10.0×10^4
192 dissolved completely in a solution pre-cooled to -12.6°C . Cai et al. [13] studied the rapid dissolution of
193 cellulose in aqueous LiOH/urea pre-cooled to -12°C and proposed a mechanism involving cleavage of
194 the chain packing of cellulose by LiOH hydrates through the formation of new hydrogen bonds. These
195 findings indicated that conformational changes of cellulose occurred in alkali solutions, even at low
196 temperatures. However, the effect of cooling on the morphological changes and solubility has not been
197 examined in detail.

198 Experiment III examined the effect of a low-temperature treatment on the morphological
199 changes in ramie. **Figure 1(b)** shows the changes that occurred during such treatment; cooling caused
200 a remarkable contraction in length and swelling in width.

201 **Figure 4** shows the changes in morphology found from Experiment III. The morphological
202 changes (open circles in **Figures 4(a) and (b)**) are similar to those found with Experiment II. This is
203 because the treatment before cooling in Experiment III was the same as that in Experiment II. The
204 morphological changes evident after cooling (crosses in **Figures 4(a) and (b)**) were quite different from
205 those found before cooling (open circles in **Figures 4(a) and (b)**). The concentration at which the
206 morphology changed shifted to lower concentration, i.e., the changes in length and width appeared at
207 $0.06 \leq [\text{NaOH}] \leq 0.12$. These morphological changes corresponded to changes in crystallinity (closed
208 circles in **Figure 3**). This suggested that the reduction in crystallinity caused the changes in
209 morphology, even under the conditions of Experiment III.

210 The morphological changes after rinsing were observed only in width, as in Experiment II.
211 The residual swelling under the cooling condition was greater than that in the absence of cooling,
212 probably because the former swelled more than the latter at the same NaOH concentration.

213

214 Changes in crystallinity line profile

215 **Figure 5(a)** shows the X-ray intensity line profiles of the ramie fibers, which corresponded to
216 the crystallinity changes shown in **Figure 3**. The changes in crystallinity profiles appeared in the same
217 $[\text{NaOH}]$ region where the morphological changes occurred; no changes appeared at $[\text{NaOH}] \leq 0.05$

218 and $[\text{NaOH}] \geq 0.12$. **Figure 5(a)** also demonstrates that structural changes occurred with the
219 transformation from cellulose I to II. The cellulose I pattern was observed for $[\text{NaOH}] \leq 0.10$, while a
220 pattern consistent with a mixture of cellulose I and II was seen for $[\text{NaOH}] = 0.11$. A higher cellulose II
221 content was noted at $[\text{NaOH}] \geq 0.12$. The pattern intensity for crystalline cellulose II at $[\text{NaOH}] \geq$
222 0.12 was weaker than that for cellulose I at $[\text{NaOH}] \leq 0.10$. This indicated a lower crystallinity.
223 Comparison of the morphological changes shown in **Figures 2(a) and (b)** with the line profiles in
224 **Figure 5(a)** clarified that a structural change of cellulose I to II caused the macroscopic changes in
225 morphology. However, the transformation from cellulose I to II hardly affected the change in ramie
226 length because there is only a slight difference in the length of their unit cells along the c axis.

227 The X-ray diffraction profiles after cooling are shown in **Figure 5(b)**. Cellulose I was found at
228 $[\text{NaOH}] \leq 0.05$, cellulose I and II co-existed at $[\text{NaOH}] = 0.07$, and cellulose II was clearly found at
229 $[\text{NaOH}] \geq 0.08$. The intensity decreased significantly in the transition region from cellulose I to II. The
230 results of both Experiments II and III indicated that changing morphology was strongly related to
231 changing crystallinity rather than to the transformation.

232 **Figure 6** shows the relationship between crystallinity before and after cooling. The plots
233 should lie on a linear as a broken line in **Figure 6**, if the NaOH treatment contributes equally to
234 de-crystallization in both cases. However, it shows clearly that the $[\text{NaOH}]$ region that induced the
235 change in crystallinity differed for the two cases, i.e., the trajectory deviated from a straight line in the
236 region of $[\text{NaOH}]$, $0.07 \leq [\text{NaOH}] \leq 0.12$.

237

238 Morphological changes and microfibril conformation

239 **Figure 7** shows the relationship between the morphology and crystallinity for samples in
240 Experiments II and III. There were strong linear correlations between the length and crystallinity,
241 and between the width and crystallinity, regardless of cooling or non-cooling and rinsing or
242 non-rinsing. This linearity was clearly evident even for the width after rinsing (closed circles in **Figure**
243 **7(b)**).

244 The results shown in **Figure 7** demonstrate that the morphological changes in ramie fiber
245 were related to crystallinity. There is a possibility that de-crystallization via NaOH treatment caused
246 two conformational changes, i.e., changes to both the cellulose chains and to the microfibrils. Our
247 interest is in the mechanism of the morphological changes, i.e., the cause of the contraction. Nakano et
248 al. [40] and Nakano [41] proposed a mechanism concerning conformational changes induced by NaOH
249 treatments.

250 The morphological changes in ramie can be understood in terms of Nakano's mechanism.
251 First, NaOH-water solution attacks the periodic defects along the microfibrils and diffuses into the
252 cross-sections. Periodic defects in microfibrils have been confirmed by a leveling-off of the degree of
253 polymerization (LODP). Nishiyama [31] reported that microfibrils have 4-5 disordered residues for
254 every 300 residues. Diffusing NaOH-water solutions creates amorphous regions. Crystalline and
255 amorphous regions might co-exist in series after some time, even though initially the amorphous
256 region is distributed. A part of the stretched cellulose chains in the crystalline microfibrils transform to
257 random conformations; hence, the dimensions contract along the microfibrils. Thermodynamically,

258 this is an entropy-increasing process. That is, the driving force for the contraction is the entropic
259 elastic force.

260 The above explanation, however, is based on the contribution of the conformational change
261 in the cellulose chains alone. Our question was whether or not the conformational changes in the
262 microfibrils alone contributed to the morphological changes. The residual swelling after rinsing
263 provided insight. As shown by the closed circles in **Figure 2(b)**, the width after rinsing did not return to
264 the initial value and the residual swelling increased with increased swelling immediately after NaOH
265 treatment, i.e., with decreased crystallinity. The changes in length and width were highly correlated
266 with crystallinity, even after rinsing (**Figure 7**). The length was not influenced by rinsing, while the
267 width was strongly affected by rinsing. It should be noted that a residual swelling after rinsing was
268 estimated at most 0.3 point. The answer to our question can be obtained by examination whether or
269 not this value in width after rinsing allows the conformational changes in microfibrils alone.

270 Consider the probable conformational change in the microfibrils alone after rinsing: crystal
271 and amorphous regions act as bonds and joints, respectively. We take up a symmetric zigzag
272 conformation with 1° bond angle as an example. The size of bond width and joint is not considered to
273 simplify our discussion. This example has a rod-like feature due to a small bond angle. If the width of
274 this conformation is larger than a residual swelling in width, the significant conformational change in
275 the microfibrils alone should hardly occur with NaOH treatment.

276 According to Nishiyama [31], the residues between periodic defects along ramie microfibrils
277 is 300, and about 250 residues remain in the crystal region even after 0.2 point of the maximum

278 decrease in crystallinity as shown in **Figure 3**. The length is approximately 125 nm when the residue
279 length is 0.52 nm and the bond angle of the β 1-4 ether linkages is not considered. Then, the increase
280 in width is $125 \sin 0.5^\circ = 1.09$ nm after the symmetric zigzag conformation with bond angle 1° . On the
281 other hand, the maximum residual swelling 0.3 is corresponding to 0.6 to 1.8 nm and the average 1.2
282 nm, setting the microfibril width before the treatment 2 to 6 nm which is the general value for higher
283 plant. The calculated value is nearly equal to the maximum residual swelling value, that is, the
284 change in width of the zigzag conformation is close to the maximum value observed in our experiment,
285 even if the bond angle is very small 1° . Consequently, significant conformational changes in the
286 microfibrils are not expected with the NaOH treatment.

287 This implies that the amorphous regions created along the microfibrils during the NaOH
288 treatment do not act as joints. Probably, the joints should have much lower flexibilities comparing
289 with the β 1-4 ether linkages of the cellulose chains which have free rotation around the bonds. Thus,
290 the conformation of the microfibrils may remain rod-like. Consequently, the morphological change is
291 mainly attributed to the change in conformation of the cellulose chains de-crystallized via NaOH
292 treatment. The schematic change is shown in **Figure 8**.

293

294

295 **Conclusion**

296 The morphology of ramie fiber treated with NaOH at various concentrations was observed
297 by EIM equipped with a CCD camera. The changing crystallinity was documented by X-ray

298 diffraction. We proposed the following mechanism for the observed changes in morphology. First, the
299 NaOH-water solution attacks attacked the periodic defects along the microfibrils and diffused into the
300 cross-sections. Second, diffusing NaOH-water solutions created amorphous regions. Crystalline and
301 amorphous regions might co-exist in series after sufficient time has passed. The straight cellulose
302 chains in the crystalline microfibrils partially transforms into random conformations, resulting in
303 contraction along the microfibrils. However, significant conformational changes in the microfibrils are
304 not expected because the joints, which are amorphous regions created by the NaOH treatment, are
305 inflexible. Consequently, the morphological change is mainly attributed to the change in conformation
306 of the cellulose chains de-crystallized via NaOH treatment.

307

308

309 **Acknowledgments**

310 The authors thank Prof. Junji Sugiyama, Research Institute for Sustainable Humanosphere,
311 Kyoto University for providing the ramie.

312

313

314 **References**

- 315 [1]. Eichhorn, S.J., Dufresne, A., Aranguren, M., Marcovich, N.E., Capadona, J.R., Rowan, S.J., Weder,
316 C., Thielemans, W., Roman, M., Renneckar, S., Gindl, W., Veigel, S., Keckes, J., Yano, H., Abe, K.,
317 Nogi, M., Nakagaito, A.N., Mangalam, A., Simonsen, J., Benight, A.S., Bismarck, A., Berglund,
318 L.A., Peijs, T. (2010) Review; current international research into cellulose nanofibers and
319 nanocomposites. *J Mater Sc* 45: 1-33.
- 320 [2]. Revol, J.-F., Goring, D.A.I. (1981) On the mechanism of the mercerization of cellulose in wood. *J*
321 *Appl Polym Sci* 16: 1275-1282.
- 322 [3]. Murase, H., Sugiyama, J., Saiki, H., Harada, H. (1988) The effect of lignin on mercerization of
323 cellulose in wood. *Mokuzai Gakkaishi* 34: 965-972.
- 324 [4]. Okano, T. and Sarko, A. (1984) Mercerization of cellulose I. X-ray diffraction evidence for
325 intermediate structures. *J Appl Polym* 29: 4175-4182.
- 326 [5]. Okano, T. and Sarko, A. (1985) Mercerization of cellulose II. Alkali-cellulose intermediates and a
327 possible mercerization mechanism. *J Appl Polym* 30: 325-332.
- 328 [6]. Hayashi, J., Yamada, T., Shimizu, Y.-L. (1989) Memory phenomenon of the original crystal
329 structure in allomorphs of Na-cellulose. In *Cellulose and Wood: Chemistry and Technology*,
330 *Proceedings of the Tenth Cellulose Conference* (C. Schuerch, ed.). New York: John Wiley and Sons,
331 pp. 77-102.
- 332 [7]. Nishimura, H., Okano, T., Sarko, A. (1991a) Mercerization of cellulose 5, Crystal and molecular
333 structure of Na-cellulose I. *Macromolecules* 24: 759-770.
- 334 [8]. Nishimura, H., Okano, T., Sarko, A. (1991b) Mercerization of cellulose 6. Crystal and molecular
335 structure of Na-cellulose IV. *Macromolecules* 24: 771-778.
- 336 [9].Fengel, D., Jakob, H., Strobel, C. (1995) Influence of the alkali concentration on the formation of
337 cellulose II. *Holzforschung* 49: 505-511.
- 338 [10]. O'sullivan, A.C. (1997) Cellulose: the structure slowly unravels. *Cellulose* 4: 173-207.

- 339 [11]. Kamide, K., Okajima, K., Kowsaka, K. (1985a) CP/MASS ¹³C NMR spectra of cellulose Solids: An
340 explanation by the intramolecular hydrogen bond concept. *Polymer J* 17: 701-706.
- 341 [12]. Kamide, K., Kowsaka, K., Okajima, K. (1985b) Determination of intramolecular hydrogen bonds
342 and selective coordination of sodium cation in alkalicellulose by CP/MASS ¹³C. *Polymer J* 17:
343 707-711.
- 344 [13]. Cai, J., Zhang, L. (2006) Unique gelation behavior of cellulose in NaOH/urea aqueous solution.
345 *Biomacromolecules* 7: 183-189.
- 346 [14]. Cai, J., Zhang, L., Chang, C., Cheng, G., Chen, X., Chu, B. (2007a) Hydrogen-bond-induced
347 inclusion complex in aqueous cellulose/LiOH/Urea solution at low temperature. *Chem Phys*
348 *Chem* 8: 1572-1579.
- 349 [15]. Cai, J., Zhang, L., Zhou, J., Qi, H., Chen, H., Kondo, T., Chen, X., Chu, B. (2007b) Multifilament
350 fibers based on dissolution of cellulose in NaOH/urea aqueous solution: structure and properties.
351 *Adv Materials* 19: 821-825.
- 352 [16]. Roy, C., Budtova, T, Navard, P., Bedue, O. (2001) Structure of cellulose – soda solutions at low
353 temperature. *Biomacromolecules* 2: 687-693.
- 354 [17]. Davidson G.F. (1934) The dissolution of chemically modified cotton cellulose in alkaline solution.
355 Part I: In solution of NaOH, particularly at T°C below the normal. *J Text Inst* 25: 174-196.
- 356 [18]. Sobue, H., Kiessing, H., Hess, K. (1934) The cellulose-sodium hydroxide-water system as a
357 function of the temperature. *Z Physik Chem B* 43: 309-328.
- 358 [19]. Watanabe, S., Kimura, K., Akahori, T. (1968) A study of mercerization of native cellulose by X-ray
359 method. *Bulletin of the Faculty of Eng. Hokkaido University* 47: 121-130.
- 360 [20]. LeMoigne N. and Navard, P. (2010a) Dissolution mechanisms of wood cellulose fibers in
361 NaOH-water *Cellulose* 17: 31-45.
- 362 [21]. LeMoigne, N., Bikard, J., Navard, P. (2010b) Rotation and contraction of native and regenerated
363 cellulose fibers upon swelling and dissolution: the role of morphological and stress unbalances.
364 *Cellulose* 17: 507-519.

- 365 [22]. Stöckmann, V.E. (1971a) Effect of pulping on cellulose structure Part I. *Tappi* 54: 2033-2037.
- 366 [23]. Stöckmann, V.E. (1971b) Effect of pulping on cellulose structure Part II. *Tappi* 54: 2038-2045.
- 367 [24]. Nakano, T. (1989a) Plasticization of wood by alkali treatment; Relationship between
368 plasticization and the ultra-structure (in Japanese). *Mokuzai Gakkaishi (Journal of the Japan*
369 *Wood Research Society)* 35: 431-437.
- 370 [25]. Nakano, T. (1989b) Plasticization of wood by alkali treatment; Effects of kind of alkali and
371 concentration of alkaline aqueous solution on stress relaxation (in Japanese). *Nihon Reorogi*
372 *Gakkaishi (Journal of the Society of Rheology, Japan)* 16: 104-110.
- 373 [26]. Ishikura, Y and Nakano, T. (2007) Contraction of the microfibrils of wood treated with aqueous
374 NaOH. *J Wood Sci* 53: 175-177.
- 375 [27]. Tanimoto, Y., Nakano, T. (2012) Stress relaxation of wood partially non-crystallized using
376 aqueous NaOH solutions. *Carbohydrate Polymers* 87: 2145-2148.
- 377 [28]. Tanimoto, Y., Nakano, T. (2013) Side-chain motion of components in wood samples partially
378 de-crystallized using aqueous NaOH solution. *Carbohydrate Polymers* 87: 2145-2148.
- 379 [29]. Voronova et al. (2004) Changes in the structure of flax cellulose induced by solutions of lithium,
380 sodium, and potassium hydroxides. *Fiber Chemistry* 36: 15-19.
- 381 [30]. Ray, D. and Sarkar, B.K. (2001) Characterization of alkali-treated jute fibers for physical and
382 mechanical properties. *J Appl Polym Sci* 80: 1013-1020.
- 383 [31]. Nishiyama, H, Kim, U., Kim, D., Katsumata, K., May, R.P., Langan P. (2003) Periodic disorder
384 along ramie cellulose microfibrils. *Biomacromolecules* 4: 1013-1017
- 385 [32]. Sao, K.P., Samantary, B, Bhattacharjee, S. (1996) X-ray line profile analysis in alkali-treated
386 ramie fiber. *J Appl Polym Sci* 60: 919-922.
- 387 [33] Mansikkamäki, P., Lahtinen, M., Rissanen, K. (2007) The conversion from cellulose I to cellulose II
388 in NaOH mercerization performed in alcohol-water systems: An X-ray powder diffraction study.
389 *Carbohyd Polym* 68: 35-43.
- 390 [34] Revol, J.F., Dietrich, A., Goring, D.A.I. (1987) Effect of mercerization on the crystallite size and

391 crystallinity index in cellulose from different sources. *Can J Chem* 65: 1724-1727.

392 [35] French, A.D., Cintron, M.S. (2013) Cellulose polymorphy, crystallite size, and the Segal
393 crystallinity Index. *Cellulose* 20: 583-588.

394 [36] Horii, F., Hirai, A., Kitamura, R. (1982) Solid-state high-resolution ^{13}C -NMR studies of
395 regenerated cellulose samples with different crystallinities. *Polym Bull* 8: 163-170.

396 [37] Miura, K., Nakano, T. (2012) T. Abstracts of the 62nd Annual meeting of the Japan Wood Research
397 Society. K16-06-1015.

398 [38]. Kamide, K., Okajima, K., Kowsaka, K. (1992) Dissolution of natural cellulose into aqueous alkali
399 solution: role of super-molecular structure of cellulose. *Polymer J* 24: 71-86.

400 [39]. Yamane, C., Saito, M., Okajima, K. (1996) Industrial preparation method of cellulose-alkali dope
401 with high solubility. *Senni Gakkaishi (Journal of the Society of Fiber Science and Technology, Japan)*
402 52: 310-317.

403 [40]. Nakano, T., Sugiyama J., Norimoto M. (2000) Contraction force and transformation of microfibril
404 with aqueous sodium hydroxide solution. *Holzforschung* 54: 315-320.

405 [41]. Nakano, T. (2010) Mechanism of microfibril contraction and anisotropic dimensional changes for
406 cells in wood treated with aqueous NaOH solution. *Cellulose* 17: 711-719.

407 [42]. Watanabe, T., Nakano, (2012) T. Abstracts of the 62nd Annual meeting of the Japan Wood
408 Research Society. A 16-02-1500.

409 [43]. Qi, H., Chang, C., Zhang, L. (2008) Effects of temperature and molecular weight on dissolution of
410 cellulose in NaOH/urea aqueous solution. *Cellulose* 15: 779-787.

411

412

413 **Captions:**

414 Figure 1. Typical morphological changes for ramie fiber treated with various NaOH-water
415 concentrations at room temperature (a) and with $[\text{NaOH}] = 0.07$ at -5°C (b).

416 Figure 2. Changes in length (L/L_0) and width (W/W_0) of ramie fiber treated with various NaOH-water
417 concentrations at room temperature (\circ , before rinsing; \bullet , after rinsing).

418 Figure 3. Changes in crystallinity of ramie fiber treated with various NaOH-water concentrations at
419 room temperature (\circ) and -5°C (\bullet).

420 Figure 4. Changes in length (L/L_0), width (W/W_0) of ramie fiber treated with various NaOH-water
421 concentrations at room temperature followed by cooling and then rinsing (\circ , before cooling; \times ,
422 after cooling; \bullet , after rinsing).

423 Figure 5. Dependence of X-ray profiles of treated samples on NaOH concentration for non-cooling and
424 cooling treatments.

425 Figure 6. Relationship between crystallinity before and after cooling for samples treated with
426 NaOH-water solution.

427 Figure 7. Crystallinity dependence of changes in length (L/L_0) and width (W/W_0) for samples treated
428 with NaOH-water solution (\circ , before rinsing; \bullet , after rinsing).

429 Figure 8. Schematic diagram showing the morphological changes in microfibrils treated with
430 NaOH-water treatment.

431

432

433

434

435

436

437

438

439

440

441

442

443

444

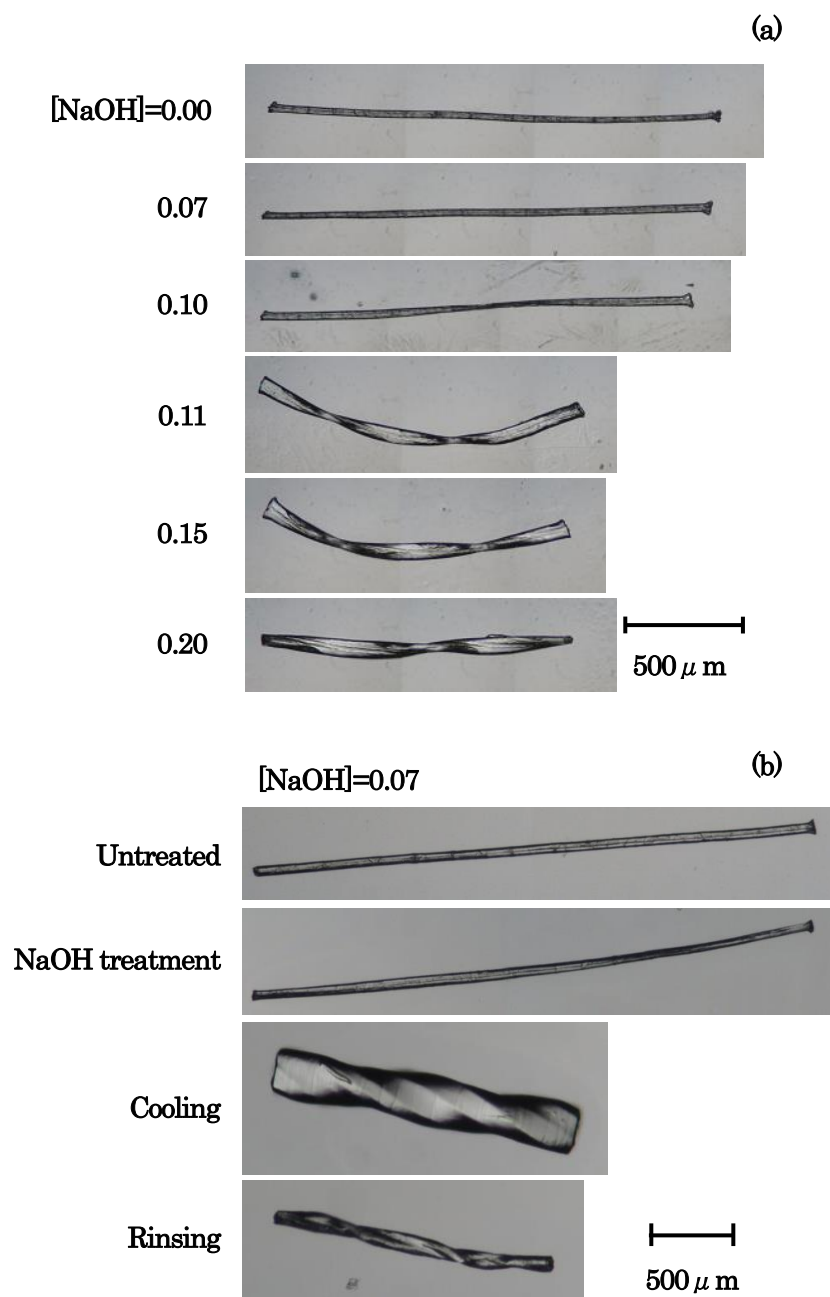
445

446

447

448 Figure 1.

449



450

451

452

453

454

455

456

457

458

459

460

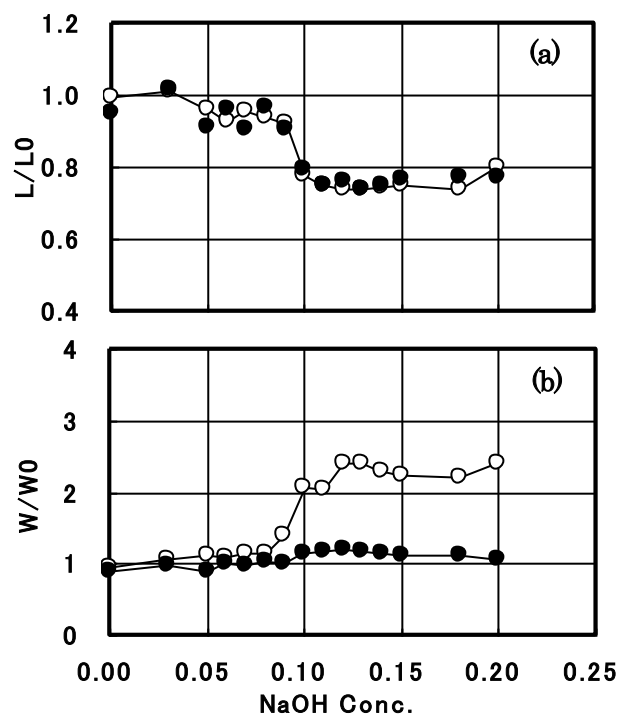
461

462

463

464 Figure 2.

465



466

467

468

469

470

471

472

473

474

475

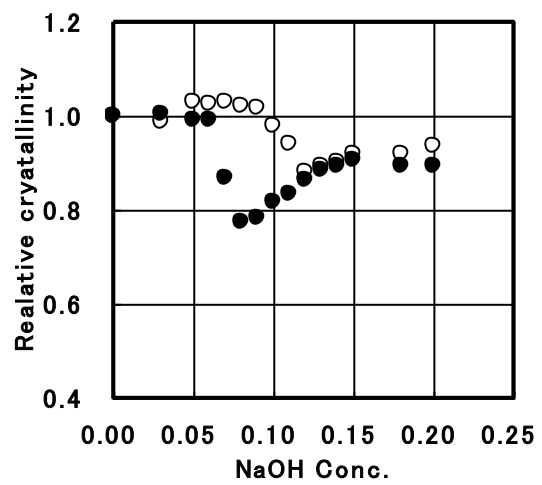
476

477

478

479 Figure 3

480



481

482

483

484

485

486

487

488

489

490

491

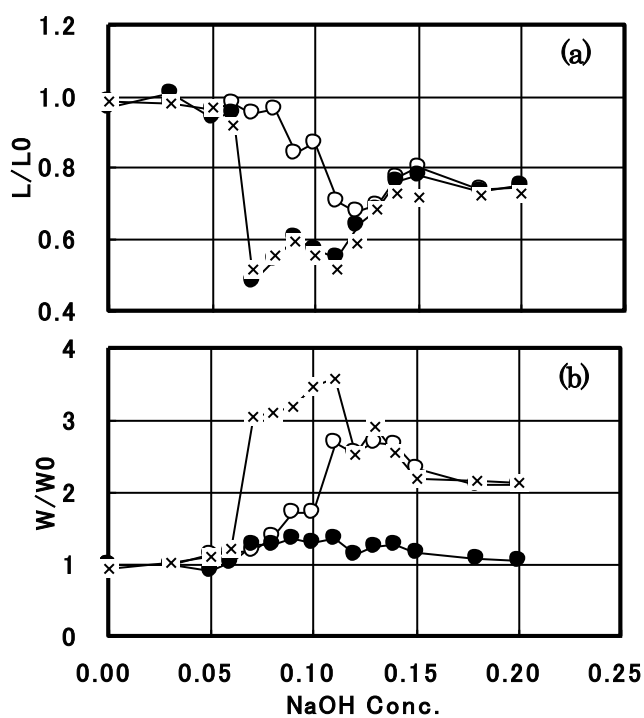
492

493

494

495 Figure 4.

496



497

498

499

500

501

502

503

504

505

506

507

508

509

510

511

512

513

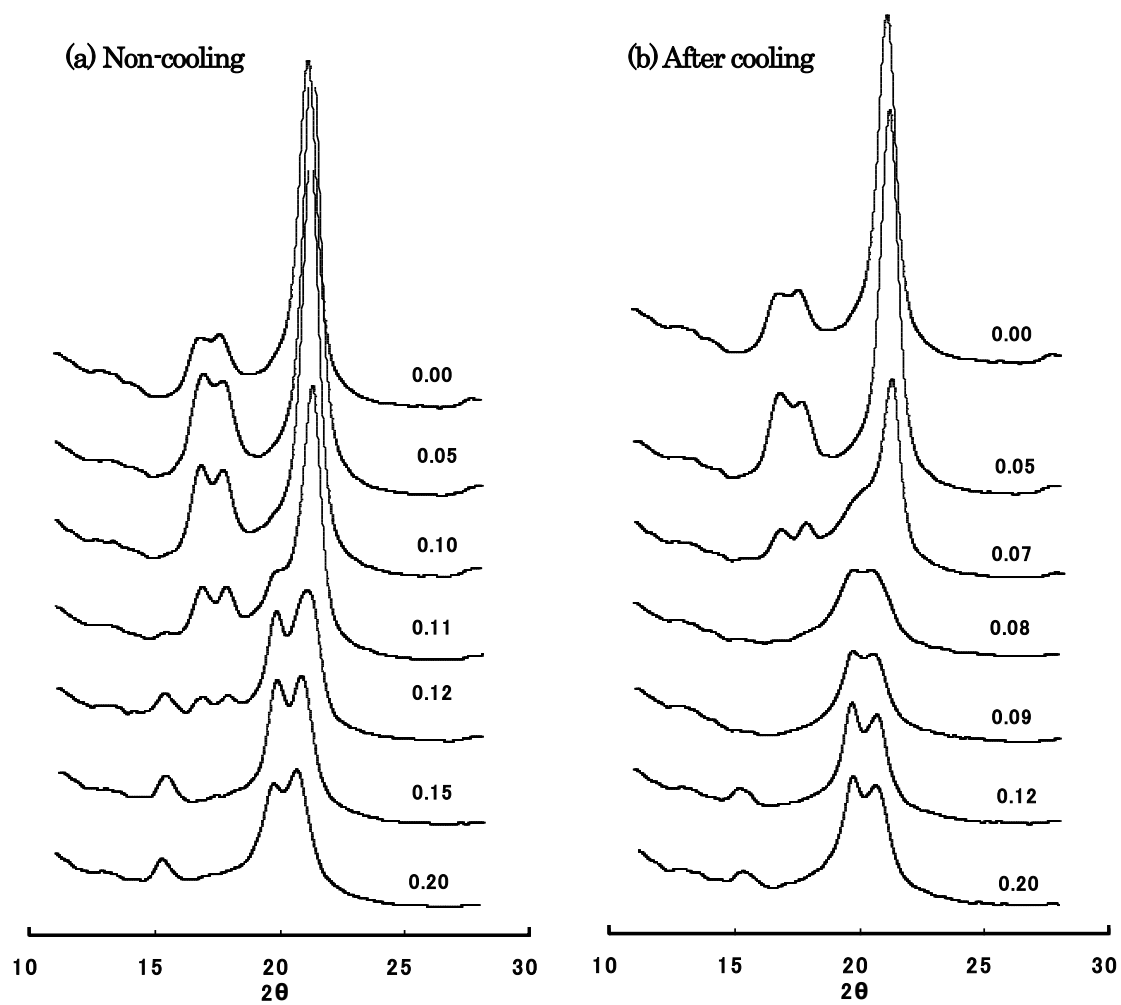


Figure 5.

514

515

516

517

518

519

520

521

522

523

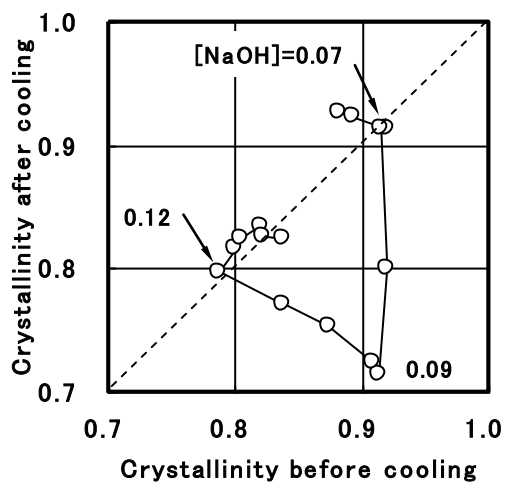
524

525

526

527 Figure 6.

528



529

530

531

532

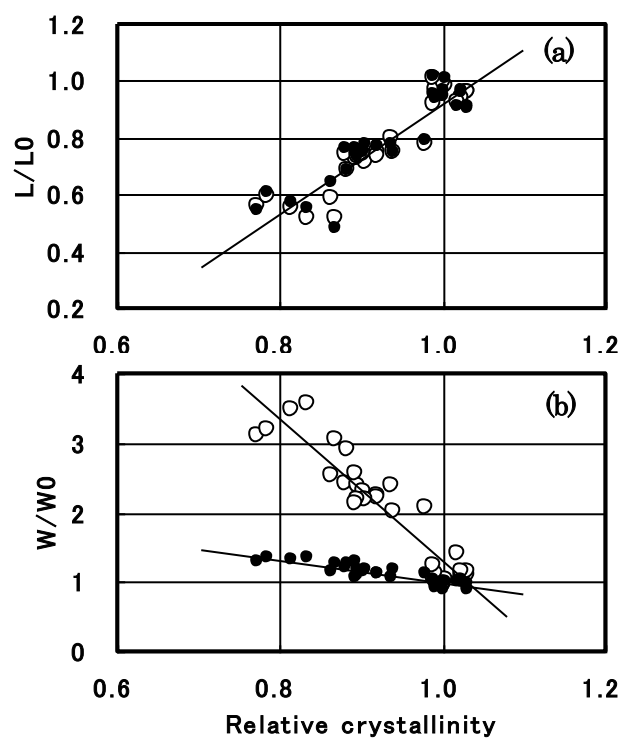
533

534

535

536

537



538

539

540

541

542

543 Figure 7.

544

545

546

547

548

549

550

551

552

553

554

555

556

557

558

559

560

561

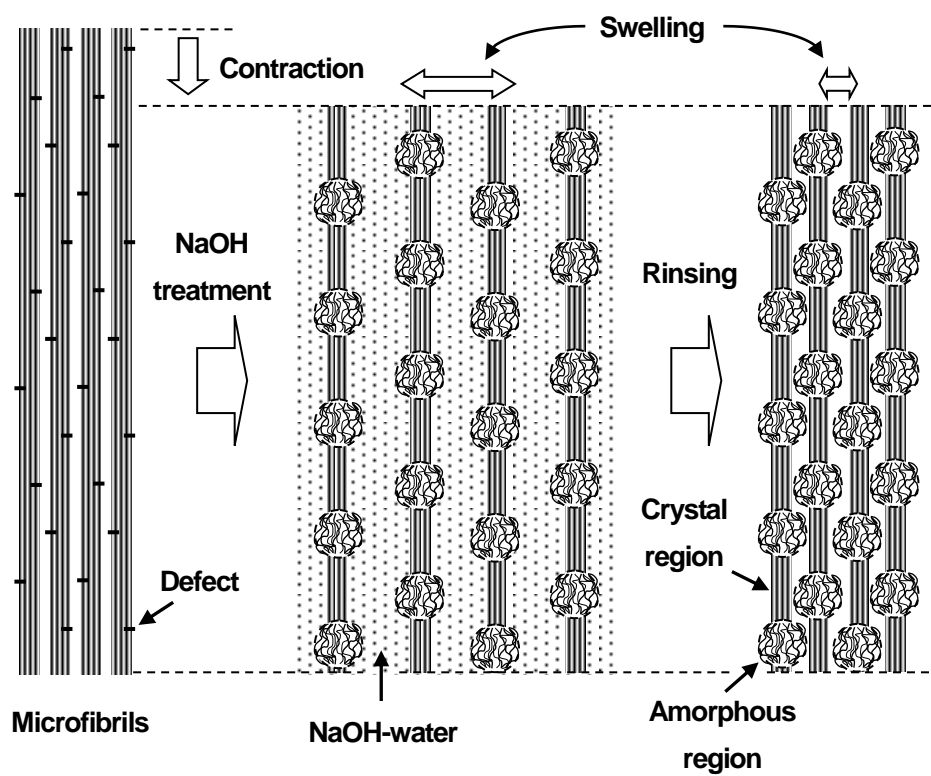


Figure 8.